Materials Transactions, Vol. 45, No. 7 (2004) pp. 2209 to 2213
Special Issue on Ultrafine Grained Structures

Formation of Nanocrystalline Structure at the Surface of Drill Hole in Steel

Yoshikazu Todaka[1], Minoru Umemoto[1], Shuji Tanaka[2] and Koichi Tsuchiya[1]

[1]*Department of Production Systems Engineering, Toyohashi University of Technology, Toyohashi 441-8580, Japan*
[2]*Fuji Univance Corporation, Kosai 431-0494, Japan*

Microstructure of martensite steel near drill hole surface was investigated. The microstructure of drill hole surface can be divided into 3 layers with depth. From top surface, nanocrystalline layer, equiaxed submicron grain layer and deformed martensite structure layer. Nano-grained layers have extremely high hardness, similar to those observed in the specimens treated by shot peening, ball milling, ball drop and particle impact deformation. The measured amount of shear strain produced by drilling was found to be an exponential function of depth from the hole surface. The amount of true strain at the hole surface region was estimated to exceed 7 which is considered to be the necessary amount of strain to produce nanocrystalline structure.

(Received January 21, 2004; Accepted March 18, 2004)

Keywords: *nanocrystallization, drilling, severe plastic deformation (SPD), steel, surface*

1. Introduction

Nanocrystalline (NC, grain size smaller than 100 nm) materials have attracted considerable scientific interests in the last decade, since these materials are expected to possess superior mechanical properties. Various severe plastic deformation processes have been proposed to produce NC materials, *e.g.* ball milling (BM),[1,2] high pressure torsion,[3,4] sliding wear[5–7] and shot peening (SP).[8–12] The necessary condition to produce NC material by deformation may be a large strain of more than about 7 in true strain.[13] This amount of strain is larger than those attained by conventional deformation processes (~5), such as rolling, drawing, extrusion. From our previous BM,[14–16] ball drop (BD),[16–18] particle impact (PI)[13] and SP[13,19,20] experiments in steels, it was found that the NC regions have the following characteristics: 1) homogeneous and featureless structure with sharp boundaries between deformed structure region, 2) extremely high hardness (8~13 GPa), 3) dissolution of cementite when it exists and 4) no recrystallization and slow grain growth by annealing.

In the present study, the nanocrystallization at the hole surface in steel by drilling was investigated. Since it is considered that a large strain is the most important condition to produce NC structure, the amount of strain at the drill hole surface of work material is evaluated. The NC regions formed at the hole surface by drilling were compared with those produced by BM, BD, PI and SP.[13–20]

2. Experimental Procedures

The materials used in the present study were a case hardening steel of SCM420H (Fe-0.17~0.23C-0.15~0.35Si-0.55~0.90Mn-0.85~1.25Cr-0.15~0.35Mo, martensite structure) and a structural steels of S45C (Fe-0.45C-0.21Si-0.69Mn, ferrite + pearlite). The drilling experiments were performed by using a sintered carbide drill with ϕ2.5 mm in diameter. The drilling parameters were peripheral cutting speed of several 10 m/min. Oil mist was used as coolant. Annealing of specimens after drilling was carried out at 873 K for 3.6 ks by sealing in a quartz tube under a pure Ar protective atmosphere. Specimens were characterized by scanning electron microscope (SEM, JEOL JSM-6500F), transmission electron microscope (TEM, Hitachi H-800 working at 200 kV) and Vickers microhardness tester (AKASHI MVK-G1). Samples for SEM observations were etched by 5% Nital. The samples for TEM observations and microhardness measurements were cut parallel to the drilling direction, as illustrated in Fig. 1. Thin foils for TEM observations were cut out from location (A)-(C) in Fig. 1 and polished electrically.

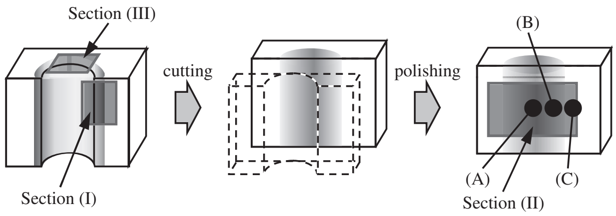

Fig. 1 Preparation procedure of samples for SEM, TEM observations and microhardness measurements after drilling experiments.

3. Results

The cross section (Section (I) in Fig. 1) of the drill hole in the SCM420H steel was observed by SEM and shown in Fig. 2. Three types of microstructure can be seen; a smooth contrast region without detectable structure near the surface of drill hole, a deformed structure (DS) region and a martensite structure region. This micrograph shows that the area more than 10 µm away from the surface of drill hole is undeformed. To examine the characteristics of grain in these regions, TEM observations were performed. Figure 3(a) shows the TEM bright field (BF) image taken from the smooth contrast region ((A) in Fig. 1). Equiaxed grains with the size of around 20 nm are seen (The smooth contrast region referred to as nanocrystalline (NC) region hereafter.). The selected area diffraction (SAD) rings (Fig. 3(b)) taken from the area of ϕ1.2 µm in Fig. 3(a) show nearly continuous rings, indicating the random orientation of the grains. The

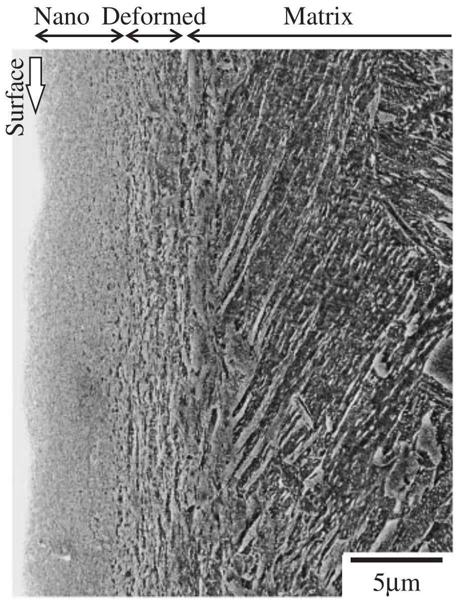

Fig. 2 The cross sectional SEM micrograph of the drill hole in the SCM420H steel. Section (I) illustrated in Fig. 1 was observed.

diffraction rings correspond to those of the bcc ferrite. (The innermost ring and other spots are from Fe_3O_4 phase, which covers the surface of the TEM sample.) The BF image (Fig. 3(c)) taken from (B) in Fig. 1 shows equiaxed grains with the size of around 100 nm. This microstructure consists of fine grains with high and low dislocation densities. The grains containing quite few dislocations, shown by arrows in Fig. 3(c), may be formed by recovery and/or recrystallization during drilling, which can be called either *in-situ*[21] or *continuous recrystallization*.[22] The BF image (Fig. 3(d)) taken at (C) in Fig. 1 shows a typical martensite structure. The hardness measurements were carried out on Section (II) in Fig. 1. Figure 4 shows the microhardness across the boundary between the NC and martensite structure regions. The hardness of the NC region is as high as 9.8 GPa, which is much higher than that of the martensite structure region (5.0 GPa). This characteristic is similar to those observed in the specimens treated by BM, BD, PI and SP.[13–20] Figure 5 shows the cross sectional SEM micrographs (Section (I) in Fig. 1) of prior NC region observed in the work material after drilling and subsequent annealing. The prior NC region keeps finer equiaxed grain structure (several 100 nm) than that of the martensite structure region even after annealing at 873 K for 3.6 ks. However, this grain size of prior NC region is much larger than those in the annealed specimens after BM, BD, PI and SP experiments.[13–16,18–20] The large recrystallized grains at the hole surface in the drilled specimen are probably due to the partial recovery during drilling because of temperature rise. The investigations of recrystallization behavior are in progress.

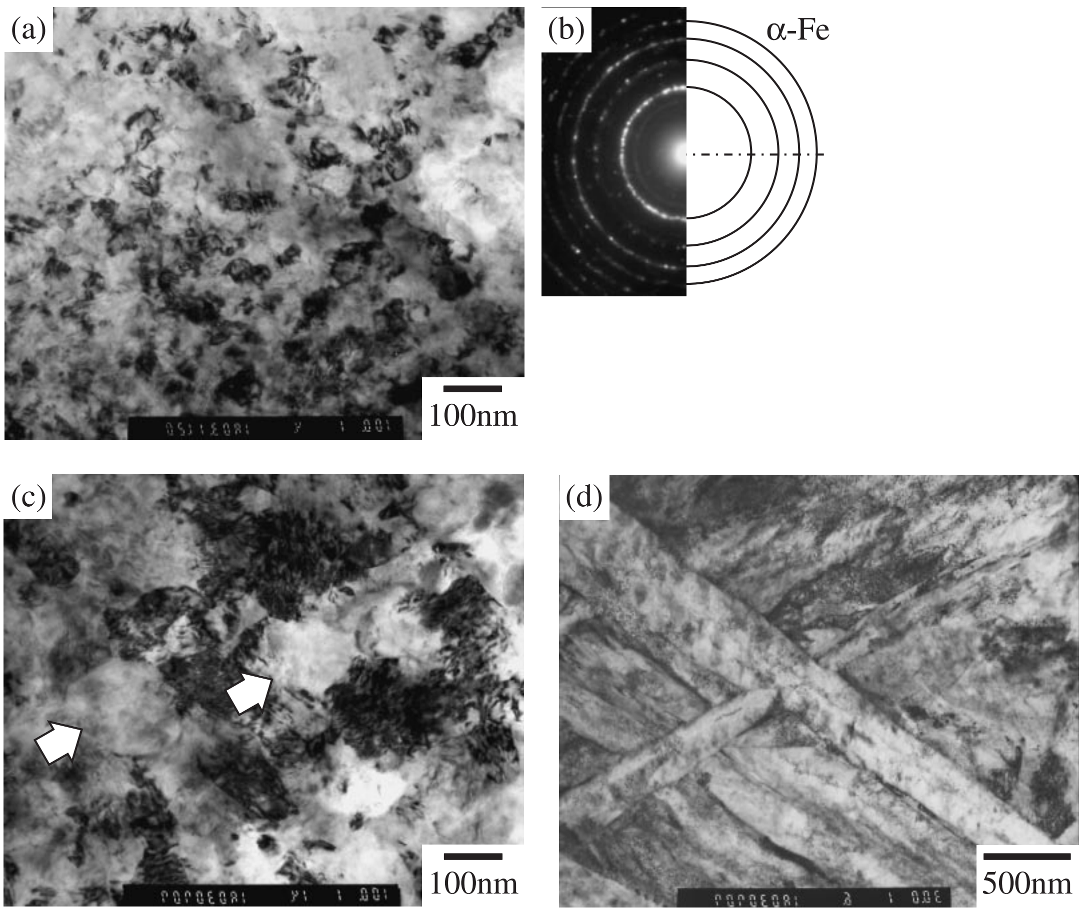

Fig. 3 The TEM images of the SCM420H steel after drilling. (a) BF image and (b) SAD rings ((ϕ1.2 μm in aperture size) taken from the NC layer ((A) in Fig. 1), (c) BF image taken at (B) in Fig. 1 and (d) BF image taken from the martensite structure region ((C) in Fig. 1).

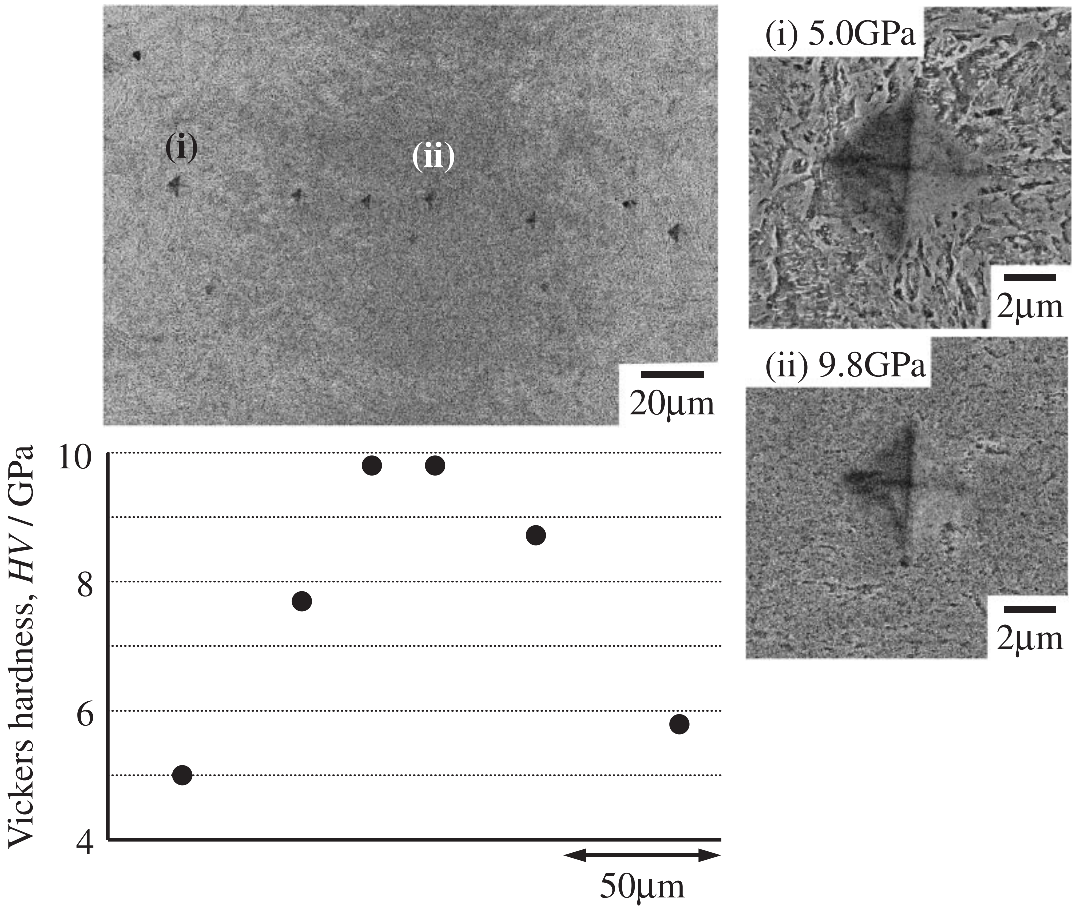

Fig. 4 The microhardness across the boundary between NC and martensite structure regions in the SCM420H steel after drilling. The microhardness of Section (II) illustrated in Fig. 1 was measured.

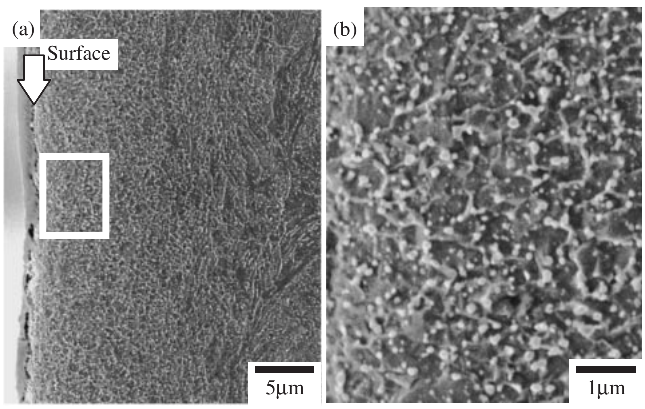

Fig. 5 The cross sectional SEM micrographs of the drill hole in the SCM420H steel after drilling and subsequent annealing. Section (I) illustrated in Fig. 1 was observed. (a) low magnification and (b) high magnification of prior NC region.

4. Discussion

In the present study, it was found that NC layer can be produced at hole surface in work material by drilling. The necessary condition to produce NC structure in steels by deformation was proposed to apply a strain lager than about 7 at temperature below $T_m/2$ (where T_m is the melting point in K).[13] However, the amount of strain given by drilling is not clear. Here, the amount of strain by drilling is evaluated.

Figure 6 shows the cross sectional SEM micrographs (Section (III) in Fig. 1) of S45C steel with ferrite and pearlite structure after drilling. Fig. 6(b) is the enlarged image of Fig. 6(a) where the cementite lamellae locate perpendicular to the hole surface before drilling. The remarkable bending of lamellar cementite to the sliding direction is seen. The curve of cementite plate can be described roughly by an exponential function of depth. The measured displacement $x(z)$ of cementite plate from the initial position by drilling are shown in Fig. 7 as a function of depth z from the top surface of drill hole. The displacement $x(z)$ decreases exponentially with the depth z from the surface, and can be expressed as

$$x(z) = x_s \cdot \exp(-k \cdot z) \tag{1}$$

where x_s is the displacement at the top surface and k is a constant. The data in Fig. 7 are replotted in Fig. 8 with $\ln(x(z))$ vs z. The straight line obtained support the assumption of eq. (1) and the line gives

$$\ln(x(z)) = \ln(x_s) - k \cdot z = \ln(14.0) - 1.46z \tag{2}$$

The shear strain $\Delta\gamma(z)$ is given by differentiating $x(z)$ by depth z, as

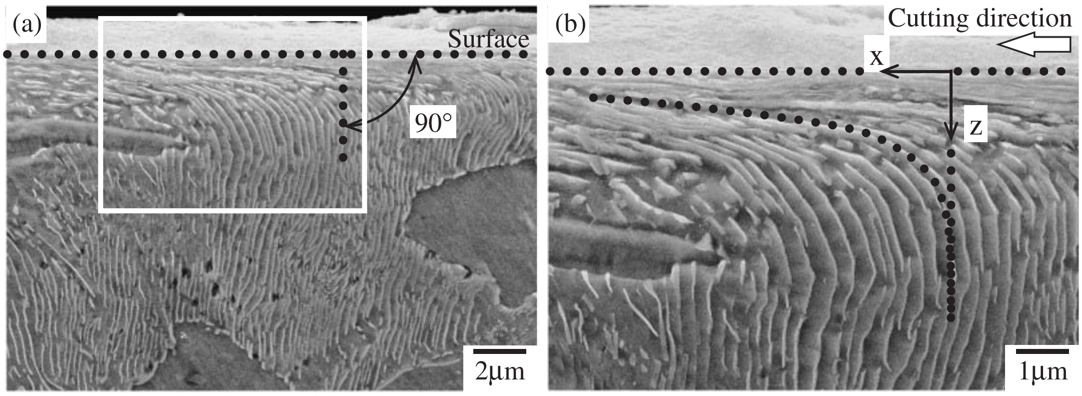

Fig. 6 The cross sectional SEM micrograph of the drill hole in the S45C steel with ferrite and pearlite structure. Section (III) illustrated in Fig. 1 was observed. (a) low magnification and (b) high magnification of the surface of drill hole.

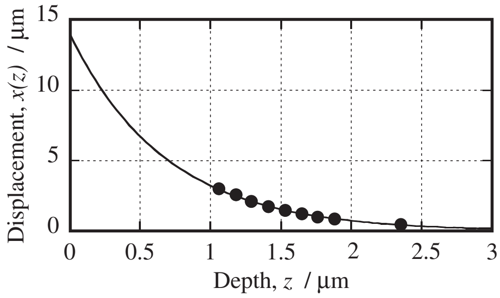

Fig. 7 The displacement $x(z)$ of cementite plate from the initial position by drilling as a function of depth z from the top surface of drill hole.

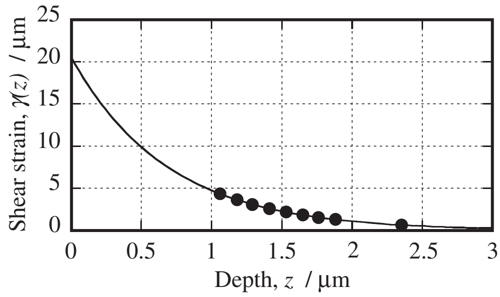

Fig. 9 The shear strain $\gamma(z)$ as a function of depth z from the top surface of drill hole.

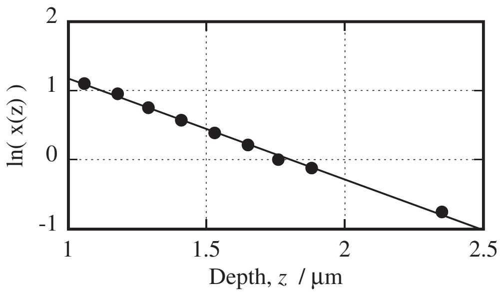

Fig. 8 The data in Fig. 7 replotted with $\ln(x(z))$ as a function of depth z from the top surface of drill hole.

$$\Delta\gamma(z) = -\frac{\partial}{\partial z}x(z) \tag{3}$$

$$\begin{aligned}\gamma(z) &= \gamma_s \cdot \exp(-k \cdot z) = k \cdot x_s \cdot \exp(-k \cdot z)\\ &= 20.4\exp(-1.46z)\end{aligned} \tag{4}$$

where γ_s is the shear strain at the top surface. $\gamma(z)$ is plotted as a function of depth z in Fig. 9. The shear strain at the top surface γ_s was estimate to be 20.4 by extrapolating the curve in Fig. 9. Thus, the shear strain is extremely large at the top surface, and it decreases rapidly with the depth from the surface. The amount of the true strain at the top surface ε_s is calculated, *i.e.*

$$\varepsilon_s = \frac{1}{\sqrt{3}}\gamma_s = 11.8 \tag{5}$$

Here, it is noteworthy that the highest strain achieved by drilling was as large as 11.8. This indicating that the strain given by drilling is large enough to produce NC structure. The thickness of the surface layer corresponding to true strain lager than 7 is calculated to be 0.36 μm from eq. (4). This is significantly smaller than that of nanocrystalline layer observed in the SCM420H steel (Fig. 2). This is due to the different in the amount of deformation and heat generation between the two steels by drilling since the initial strength and work-hardening rate of these steels are different.

5. Conclusions

Microstructure evolution of drill hole surface in martensite steel was investigated. In all the drilled holes, the equiaxed nanocrystals with grain size of a few 10 nm were observed at the top surface regions. The depth of nanocrystalline layers was several μm. The nanocrystalline layers have extremely high hardness, similar to those observed in the specimens treated by shot peening, ball milling, ball drop and particle impact deformation.

Acknowledgements

This study is financially supported in part by the Grant-in-Aid by the Japan Society for the Promotion of Science and the ISIJ Research Promotion Grant by the Iron and Steel Institute of Japan (ISIJ).

REFERENCES

1) C. H. Moelle and H. J. Fecht: NanoStruct. Mater. **6** (1995) 421–424.
2) S. Takaki and Y. Kimura: J. Jpn. Soc. Powder Powder Metal. **46** (1999) 1235–1240.
3) A. V. Korznikov, Y. V. Ivanisenko, D. V. Laptionok, I. M. Safarov, V. P. Pilyugin and R. Z. Valiev: NanoStruct. Mater. **4** (1994) 156–167.
4) R. Z. Valiev, Y. V. Ivanisenko, E. F. Rauch and B. Baudelet: Acta Mater. **44** (1996) 4705–4712.
5) P. Heilmann, W. A. T. Clark and D. A. Rigney: Acta Metall. **31** (1983) 1293–1205.
6) D. A. Rigney, M. G. S. Naylor and R. Divakar: Mater. Sci. Eng. **81** (1986) 409–425.
7) D. A. Hughes, D. B. Dawson, J. S. Korellis and L. I. Weingarten: Wear **181–183** (1995) 458–468.
8) I. Altenberger, B. Scholtes, U. Martin and H. Oettel: Mater. Sci. Eng. A **264** (1999) 1–16.
9) X. Y. Wang and D. Y. Li: Wear **255** (2003) 836–845.
10) G. Liu, S. C. Wang, X. F. Lou, J. Lu and K. Lu: Scr. Mater. **44** (2001) 1791–1795.
11) N. R. Tao, Z. B. Wang, W. P. Tong, M. L. Sui, J. Lu and K. Lu: Acta Mater. **50** (2002) 4603–4616.
12) H. W. Zhang, Z. K. Hei, G. Liu, J. Lu and K. Lu: Acta Mater. **51** (2003) 1871–1881.
13) M. Umemoto, Y. Todaka and K. Tsuchiya: Mater.Trans. **44** (2003) 1488–1493.
14) J. Yin, M. Umemoto, Z. G. Liu and K. Tsuchiya: ISIJ Int. **41** (2001) 1389–1396.
15) Y. Xu, M. Umemoto and K. Tsuchiya: Mater. Trans. **43** (2002) 2205–2212.
16) Y. Todaka, M. Umemoto and K. Tsuchiya: ISIJ Int. **42** (2002) 1429–1436.
17) M. Umemoto, B. Huang, K. Tsuchiya and N. Suzuki: Scr. Mater. **46** (2002) 383–388.
18) M. Umemoto, X. Hao, T. Yasuda and K. Tsuchiya: Mater. Trans. **43** (2002) 2536–2542.
19) Y. Todaka, M. Umemoto, Y. Watanabe and K. Tsuchiya: J. Japan Inst. Metals **67** (2003) 690–696.
20) Y. Todaka, M. Umemoto and K. Tsuchiya: Mater. Trans. **45** (2004) 376–379.
21) N. Tsuji, R. Ueji, Y. Ito and Y. Saito: Proc. of 21st Riso Int. Sym. on Mater. Sci. (2000) 607–616.
22) A. Belyakov, T. Sakai and H. Miura: Mater. Trans., JIM **41** (2000) 476–484.